


RESEARCH

Open Access



PolSAR image classification based on Laplacian Eigenmaps and superpixels

Haijiang Wang^{1,2*} , Jinghong Han¹ and Yangyang Deng¹

Abstract

This paper proposes a method of polarimetric synthetic aperture radar (PolSAR) image classification using improved superpixel segmentation and manifold learning. Firstly, a 27-dimension polarimetric feature space is extracted by simple arithmetic operations of polarimetric parameters and polarimetric target decomposition. Secondly, Laplacian Eigenmap (LE) algorithm is used to reduce the dimension of the 27-dimension polarimetric features. This algorithm can reduce redundant information in feature space and extract the main information. Then, the paper uses SVM which has the best classification performance to classify the low-dimension PolSAR data for the first time. And then, the superpixel segmentation is obtained by improving SLIC algorithm. At last, the majority voting principle is used to classify the superpixel blocks, which is the second classification and final classification of PolSAR data.

Keywords: Dimension reduction, SVM, Superpixels, Majority voting principle

1 Introduction

Polarimetric synthetic aperture radar (PolSAR) is an active microwave remote sensing imaging radar, which emits electromagnetic pulses with different polarimetric states and then receives echoes reflected by ground objects, so as to obtain the scattering characteristics of the ground object target objects. PolSAR imaging principle and conventional optical remote sensing imaging principle is essentially different. PolSAR data is different from the common optical image in characteristic performance; moreover, it contains different information. The polarimetric synthetic aperture radar can be used to classify polarimetric SAR images based on the obtained scattering characteristics.

According to scatter characteristics, PolSAR image classification methods can be divided into two categories: the classification method based on statistical model and the polarimetric target decomposition method. The mathematical methods based on the statistical method of statistical model are statistical modeling and Bayes theory [1]. Whether the statistical model is correctly established or not determines the accuracy of the

classification method. The polarimetric target decomposition method can classify the PolSAR image without the probability distribution of data [2], such as H/a, H/A/α decomposition [3], Pauli decomposition [4], and Krogger decomposition [5].

There are some other ways to classify PolSAR images from other perspectives.

According to whether or not selecting the training samples with class labels in advance, the PolSAR target classification method can be divided into supervised classification [6–15] and unsupervised classification [16–23]. The supervised classification requires the selection of labeled training samples and the handling of unlabeled PolSAR image data based on the characteristics of the sample. For unsupervised classification, the required prior knowledge is our empirical information and model description of the backscatter characteristics of the feature.

The most common use of PolSAR in supervised classification is based on the statistical distribution of Bayes distribution and Wishart distribution. The maximum likelihood method based on the complex Gaussian distribution proposed by Kong and others is the embryonic form use of Bayes of the PolSAR classification. Due to the influence of speckle, Lee and others proposed a multi-look ML classification based on the Wishart distribution. Many subsequent studies were based on the above classification model.

* Correspondence: whj@cuit.edu.cn

¹College of Electronic Engineering, Chengdu University of Information Technology, Chengdu, Sichuan 610225, China

²CMA Key Laboratory of Atmospheric Sounding, Chengdu, Sichuan 610225, China

In the whole process of the unsupervised classification, there is no classification of sample participation, and the common used algorithms are K-Means and ISODATA.

At present, the use of machine learning to classify PolSAR images has become the mainstream method, such as classification based on neural networks and fuzzy clustering [24], classification based on neural networks and principal component analysis [25], and classification based on Support Vector Machine [26].

There are several problems in the above classification method: Firstly, in some methods, only a little polarimetric information has been used. Secondly, in some methods, much polarimetric information has been used to deal with the polarimetric data; however, the high-dimension data can only be reduced to the human-defined low dimension in these methods. Whether the polarimetric data will be lost or not during the dimension reduction has not been considered. Thirdly, many classification methods are based on the pixels, but when the impact of noise is significant, it can easily lead to wrong classifications.

The method proposed in this paper can solve the above problems effectively. Firstly, 27-dimension polarimetric information has been used to classify, both the arithmetic parameters extracted by the polarimetric parameters and the polarimetric parameters after the polarimetric target being decomposed. The 27-dimension polarimetric information basically includes all the information of PolSAR, and it overcomes the fact that some polarimetric features extracted in some methods are only a few. Secondly, the maximum likelihood estimation (MLE) method is used to estimate the intrinsic dimension of the data. This method preserves the polarimetric information and reduces the data dimension. Thirdly, the combination of superpixel classification and the use of the majority of voting principle can effectively inhibit the coherent noise on the classification. What is more, the classification result is more accurate.

The rest of this paper is organized as follows. The second part is mainly about the data preprocessing, and the third part is mainly about feature extraction and dimension reduction. Moreover, the fourth part is mainly about classification based on SVM and superpixels, and the fifth part is mainly about the experimental result and analysis. At last, the sixth part is mainly about conclusion.

2 Preprocessing of polarimetric SAR data

According to the original data of PolSAR, the scattering matrix of each pixel point of PolSAR image can be obtained.

$$S = \begin{bmatrix} s_{hh} & s_{hv} \\ s_{vh} & s_{vv} \end{bmatrix} \quad (1)$$

The two target scattering vectors are respectively

$$K_L = (s_{hh} \ s_{hv} \ s_{vv})^T$$

$$K_P = \frac{1}{\sqrt{2}} (s_{hh} + s_{vv} \ s_{hh} - s_{vv} \ 2s_{hv})^T$$

According to the upper expression, the polarimetric covariance matrix C and polarimetric coherence matrix T can be obtained.

$$C = \langle K_L K_L^H \rangle \quad (2)$$

$$T = \langle K_P K_P^H \rangle \quad (3)$$

The characteristic parameters needed in this paper can be obtained by using the above polarimetric covariance matrix C and the polarimetric coherence matrix T .

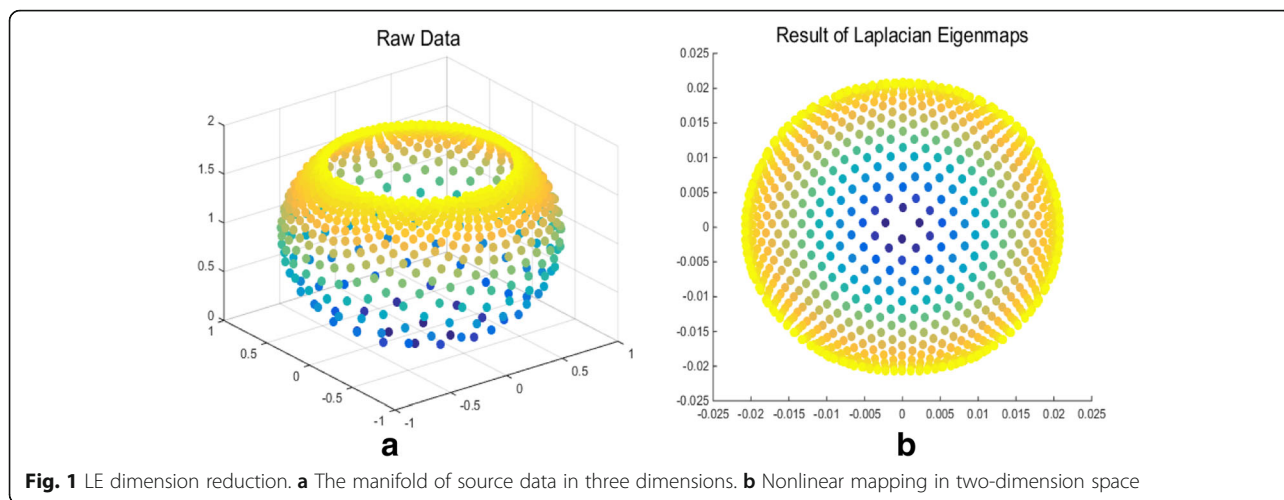
3 Polarimetric features and LE algorithm

3.1 Polarimetric features extraction

In this paper, according to [27], the 27 polarimetric parameters are extracted for each pixel of the PolSAR image, as shown in Table 1. The first 11 polarimetric features are the polarimetric parameters extracted by performing simple arithmetic operations. Its advantage is that the calculation is simple, and it can reflect some polarimetric information. The latter 16 polarimetric parameters are the polarimetric parameters after polarimetric target decomposition, and

Table 1 Twenty-seven feature parameters

Features	Expression
Span	$ s_{hh} ^2 + 2 s_{hv} ^2 + s_{vv} ^2$
Amplitude of HH-WV correlation coefficient	$\frac{ \langle s_{hh} s_{vv}^* \rangle }{\sqrt{ s_{hh} ^2 s_{vv} ^2}}$
Ratio of HV/WV (db)	$10 \log(s_{hv} ^2 / s_{vv} ^2)$
Co-polarized ratio (db)	$10 \log(s_{vv} ^2 / s_{hh} ^2)$
Cross-polarized ratio (db)	$10 \log(s_{hv} ^2 / s_{hh} ^2)$
Co-polarized HH backscattering coefficient	$\langle s_{hh} s_{hh}^* \rangle$
Co-polarized WV backscattering coefficient	$\langle s_{vv} s_{vv}^* \rangle$
Co-polarized HV backscattering coefficient	$\langle s_{hv} s_{hv}^* \rangle$
Phase of HH-WV	$\arg(\langle s_{hh} s_{vv}^* \rangle)$
Phase of HH-HV	$\arg(\langle s_{hh} s_{hv}^* \rangle)$
Phase of HV-WV	$\arg(\langle s_{hv} s_{vv}^* \rangle)$
Pauli decomposition	$ a ^2, b ^2, c ^2$
Krogager (SDH) decomposition	k_s, k_d, k_h
Cloud decomposition	H, ∂, A
Freeman-Durden decomposition	P_s, P_d, P_v
Yamaguchi decomposition	f_h, f_s, f_d, f_v



these polarimetric parameters can describe the scattering information and geometrical structure information of the target [28].

Extracted features include scattering coefficient, polarization ratio, total power, phase, Pauli decomposition, Krogager decomposition, Cloud decomposition, Freeman decomposition, and Yamaguchi decomposition. Among them, the Pauli decomposition provides three scatter intensities, and the Krogager decomposition provides the three components of three scattering. Cloud decomposition provides scattering entropy, scattering angle, and inverse entropy. Moreover, the Freeman decomposition provides three scattered powers, and the Yamaguchi decomposition provides four scattering mechanisms.

3.2 LE algorithm

The dimension reduction methods can be divided into two categories: linear method and nonlinear method. In this paper, the MLE algorithm is used to compute the intrinsic dimension of the above 27-dimension polarimetric parameters in low dimensions. The MLE method means obtaining the maximum likelihood estimation of the intrinsic dimension by establishing the likelihood function between the nearest neighbors. In some articles, the dimension after data reduction is

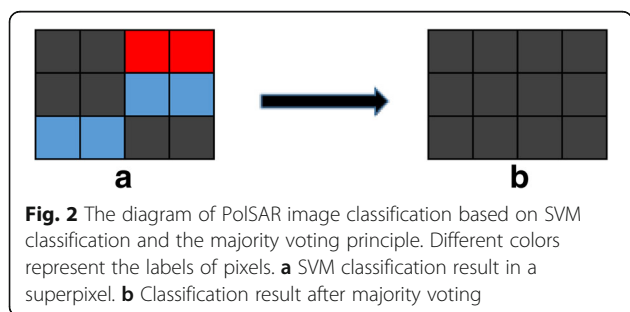
set arbitrarily, so it will inevitably cause the information loss. The MLE method can preserve the essential features of the original data in the maximum extent and can make the original data be expressed in low dimensions. LE algorithm is used to reduce the dimensions, and this approach can make high-dimension polarimetric features to be represented in low dimensions while retaining the main polarimetric information. It can be seen that this method can make full use of the polarimetric information and reduce the computational complexity of the subsequent processing. LE algorithm adopts local nonlinear method, and compared with the linear method, it can better express the real corresponding relation between the data. What is more, LE algorithm has low computational complexity and is often used to deal with the data of PolSAR image.

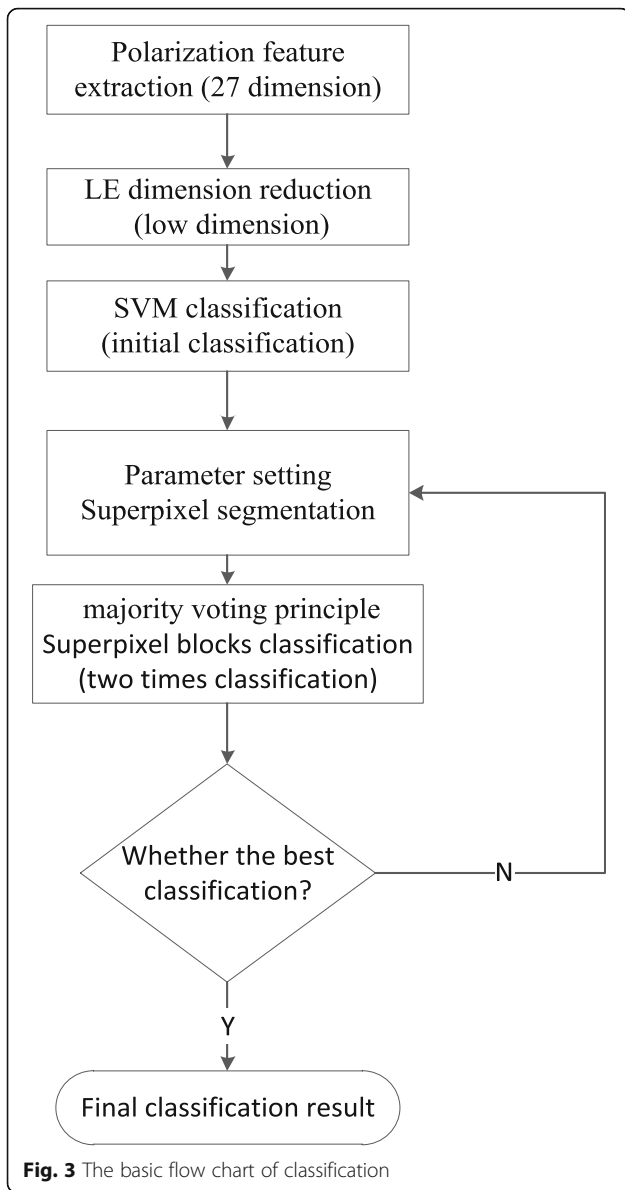
Let $X = \{x_1, x_2 \dots x_N\} \in R^{D \times N}$, where C represents the dimension of X and N represents the number of data in the X . Low dimension Y which is embedded in high-dimension X space can be found when using the LE algorithm, that is $Y = \{y_1, y_2 \dots y_N\} \in R^{D_r \times N}$. Among the expressions, N represents the number of data in the X and $D_r < D$, where D_r represents the dimension of Y .

The objective function of the LE algorithm is to minimize the following cost function, and it can ensure that the adjacent sample points are still neighbors after projection.

$$\min \sum_{ij} \left\| y_i - y_j \right\| W_{ij} \tag{4}$$

where $W_{ij} = e^{-\frac{\|x_i - x_j\|^2}{t}}$, and it reflects the relationship between samples. In order to ensure that the above function have only one solution, the scaling





normalization condition must be added. Then, the objective function changes into

$$\arg \min(YLY^T) \tag{5}$$

where L is Laplacian matrix, and $L = D - W$, D_{ii} is the diagonal matrix, and $D_{ii} = \sum_j W_{ij}$. The above function can be transformed into a generalized eigenvalue problem, that is

$$LY = \lambda DY$$

The lower dimension embedding Y takes the eigenvectors of the corresponding eigenvalues of the Laplacian matrix

$$Y = \{y_1, y_2 \dots y_N\} \in R^{D_r \times N} \tag{6}$$

The dimension reduction process is shown in Fig. 1. Figure 1a, b shows the raw data and the data after dimension reduction, respectively, by using the LE algorithm.

4 Classification based on SVM and superpixels

4.1 Support vector machine

The function of the support vector machine (SVM) is to use the hyperplane to separate each category. SVM theory is proposed by Vapnik and Cortes in 1995, and it is used to solve the problem of pattern recognition problem. At that time, SVM belonged to a linear classification model, and then, Boser, Guyon, and Vapnik introduced the kernel function, and they proposed non-linear SVM. SVM is a new learning machine built on VC (Vapnik-Chervonenkis) dimension and structural risk minimum principle of SLT, and it is mainly used for classification and regression analysis. SVM has peculiar advantages in solving nonlinear and high-dimension pattern recognition, and it has better generalization ability than that of the general learning machine.

Suppose that (x_i, y_i) , where $i = 1, 2, \dots, n$ denote a linear separable sample set, and $x \in R^d$, $y \in \{+1, -1\}$. Linear discriminant function in D dimension space is $g(x) = wx + b$, and the classification surface function is $wx + b = 0$. Make all samples satisfy $|g(x)| \geq 1$ by sample normalization, that is, the nearest sample of distance classification surface satisfies that $|g(x)| = 1$. Thus, the classification interval is equal to $\frac{1}{2} \|w\|$. Therefore, when the $\|w\|$ (or $\|w\|^2$) minimum and $y_i(wx_i + b) - 1 \geq 0$, where $i = 1, 2, \dots, n$ are satisfied, the classification surface is the optimal classification surface.

The optimal classification problem can be transformed into a constrained optimization problem as follows:

$$\min \text{se} \phi(w, b) = \frac{1}{2} \|w\|^2 \tag{7}$$

$$\text{st. } y_i(x_i \cdot w + b) - 1 \geq 0 \quad i = 1, 2, \dots, l \tag{8}$$

Therefore, the optimal classification function can be obtained as follows:

$$f(x) = \text{sgn}\{w^* \cdot x + b^*\} = \text{sgn}\left\{\sum_{i=1}^k a_i^* y_i(x_i \cdot x) + b^*\right\} \tag{9}$$

where a^* and b^* are the parameters that define the hyperplane.

When the data are linearly non-separable, a relaxation term $\xi_i \geq 0$ can be added to the constraint condition as follows:

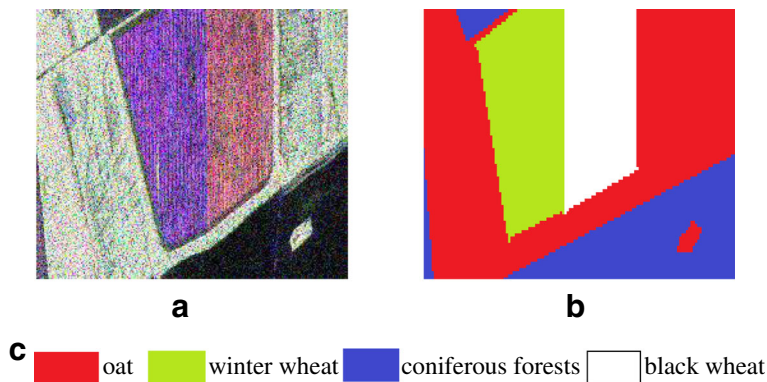


Fig. 4 The PolSAR image and truths plots in Foulum. **a** The color image of the Pauli decomposition of RGB. **b** The ground reference map. **c** The image of colored objects

$$\text{st. } y_i(x_i \cdot w + b) - 1 + \xi_i \geq 0 \quad i = 1, 2, \dots, l \quad (10)$$

Change the target to solve the minimum value of $\frac{1}{2} \|w\|^2 + C(\sum_{i=1}^n \xi_i)$, where C is a constant and $C > 0$.

The nonlinear classification can be realized by using proper kernel function $K(x_i, x_j)$ in the best classification plane, while its computational complexity will not increase [11]. The corresponding classification function will change as follows:

$$f(x) = \text{sgn} \left\{ \sum_{i=1}^k a_i^* y_i K(x_i, x) + b^* \right\} \quad (11)$$

And this is the SVM method.

The several frequently used kernel functions are linear kernel, polynomial kernel, RBF kernel, and Sigmoid kernel. The linear kernel is mainly used in linearly separable situation. The polynomial kernel can map low-dimension input space to high-dimension feature space. However, there are many parameters in polynomial kernel. When the order of polynomial is high, the element value of kernel matrix tends to be infinite or infinitesimal. The computational complexity will be too large to calculate. RBF kernel is a kind of kernel function with

strong locality, and it can map a sample into a more higher dimension space. It is the most widely used kernel. Whether or not the amount of the samples are large or small, it has great performance. And comparing with polynomial kernel, the parameter of RBF kernel is fewer. Therefore, SVM uses RBF kernel preferential in the majority of cases. The non-positive semi-definiteness of Sigmoid kernel makes its application limited. So, SVM selects RBF kernel in this paper.

4.2 Improvement of SLIC algorithm

The original PolSAR image has huge amounts of data, but the subsequent computation of the data can be greatly reduced by using the superpixels method. At the same time, superpixels can provide adaptive neighborhood information and reduce the influence of speckle on PolSAR image. At present, various superpixel generation algorithms are widely used in dealing with optical image, such as watershed algorithm [29], mean shift algorithm [30], and K-mean algorithm [31].

With the technology development for obtaining remote sensing data, the resolution of remote sensing image is increasing. While the resolution has improved,

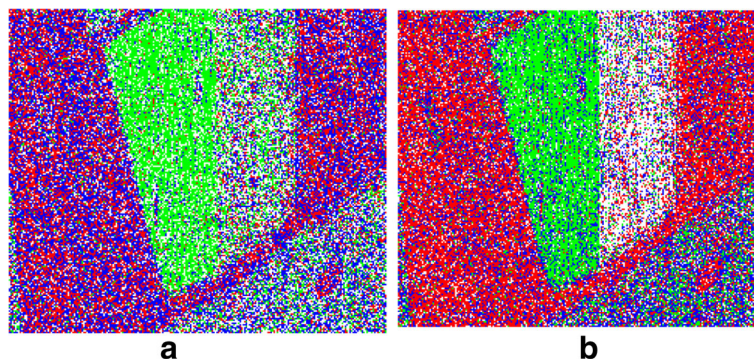
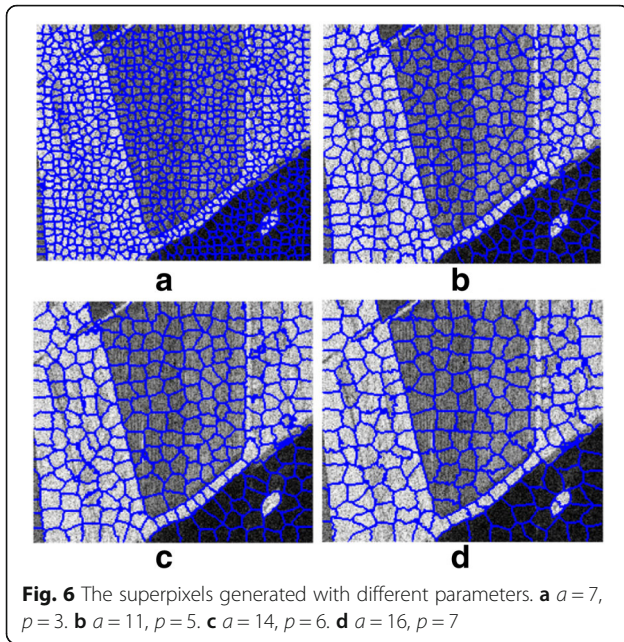
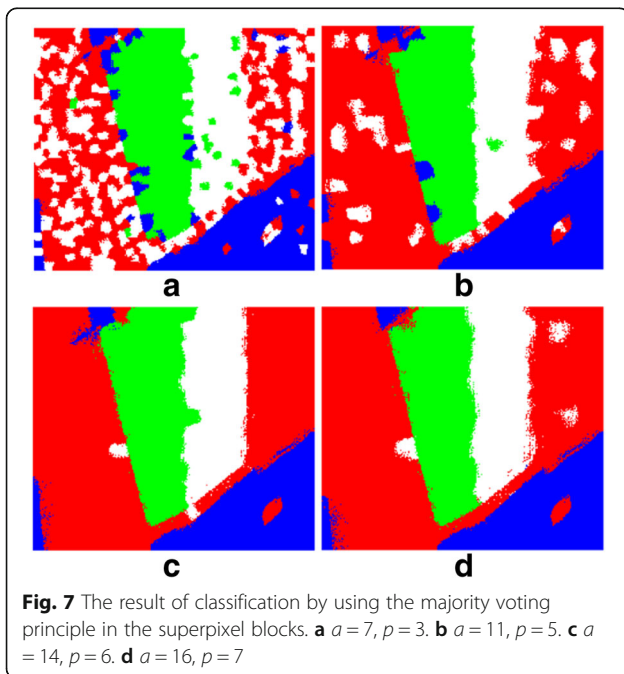


Fig. 5 The result of SVM classification. **a** The SVM classification of three polarimetric parameters. **b** The SVM classification of polarimetric parameters after reducing dimension



the amount of remote sensing image data and the redundant information is also increasing, and it is not conducive to the processing of remote sensing image. However, the introduction of superpixels can solve those problems effectively, so the application of superpixels in remote sensing image is also increasing. The superpixel blocks generated by the SLIC method are more suitable for the boundary than other methods by comparing the effects of different superpixels. Therefore, the method based on SLIC superpixel generation has been chosen to improve the effect in this paper.



The general steps of the SLIC algorithm are as follows: Firstly, initialize the seed points (clustering centers). Secondly, select the center of the superpixels. The choice is based on the spatial distance d_s and the $l\alpha\beta$ color space distance d_c between pixels and superpixels.

$$d_s(i, j) = \left((x_j - x_i)^2 + (y_j - y_i)^2 \right)^{\frac{1}{2}} \quad (12)$$

$$d_c(i, j) = \left((l_j - l_i)^2 + (\alpha_j - \alpha_i)^2 + (\beta_j - \beta_i)^2 \right)^{\frac{1}{2}} \quad (13)$$

$$D_{\text{SLIC}}(i, j) = \left(d_c^2(i, j) + \left(\frac{d_s(i, j)}{S_{\text{max}}} \right) \eta^2 \right)^{\frac{1}{2}} \quad (14)$$

where N_s is the maximum spatial distance within class, and the η is the weight.

Finally, update the center of the superpixels and iterative optimization.

Because the SLIC algorithm is used to deal with $l\alpha\beta$ color spaces, it cannot deal with PolSAR image. The color distance of optical image d_c should be transformed into gray scale as follows:

$$d'_c(i, j) = \left((g_j - g_i)^2 \right)^{\frac{1}{2}} \quad (15)$$

$$D_{\text{SLIC}}(i, j) = \left(d_c'^2(i, j) + \left(\frac{d_s(i, j)}{S_{\text{max}}} \right) \eta^2 \right)^{\frac{1}{2}} \quad (16)$$

where g_i is the grayscale value of the i th pixels.

4.3 The majority voting principle

SVM classifies polarimetric information with the single pixel without considering properties of adjacent pixels. The way proposed in this paper makes the classification more accurate by making full use of superpixels and information of the surrounding pixels [15]. The way to use the majority voting principle to classify superpixel blocks is as follows:

Firstly, each superpixel block is considered as a set, and the pixels in the set are classified by SVM to obtain the multiple labels.

Secondly, count the number of different labels in the superpixel blocks. The label with the largest number is the label of this set. Finally, the purpose to classify the superpixel blocks is achieved. The diagram is shown in Fig. 2, and each small box represents a pixel, while the large box represents a superpixel block.

The basic flow chart of classification is shown in Fig. 3.

5 The result and analysis of the experiment

The data used in the paper is the full PolSAR data in C band. The data was obtained from the EMISAR system

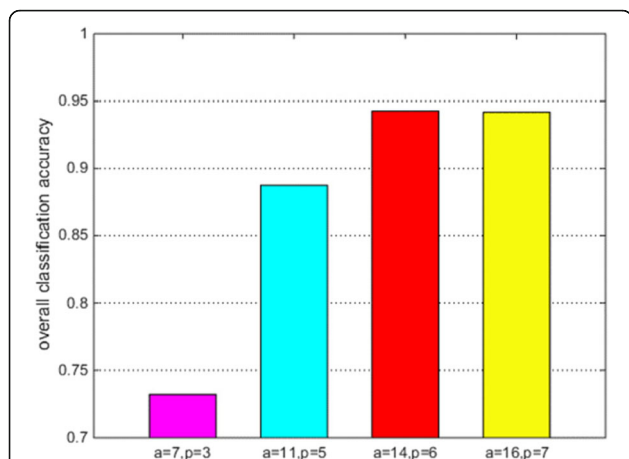


Fig. 8 The OA of classification corresponding to different superpixel generation parameters

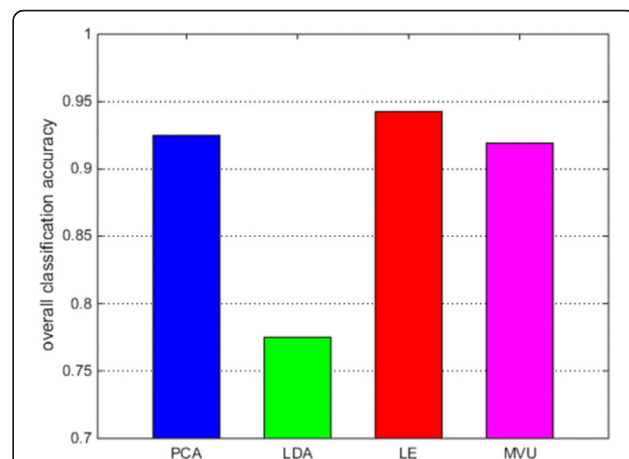


Fig. 10 The OA of classification with different dimension reduction methods corresponding to Fig. 9

in the area of Foulum in Denmark in April of 1988. In this paper, the size of experimental area is 211×244 . The RGB reference map after Pauli decomposition and ground reference map are shown in Fig. 4a, b, respectively. The image contains four types of ground features: oats, winter wheat, coniferous forests, and black wheat.

5.1 The result of SVM classification

Ten percent of each class of data were selected as training samples, and all data were used as test samples. SVM is used to classify the data with only three polarimetric parameters and the data with polarimetric parameters after reducing dimension, respectively. In this

paper, the MLE is used to estimate the intrinsic dimension of the 27-dimension polarimetric feature information. Finally, the intrinsic dimension of five dimensions has been obtained. In this paper, five cross-validation methods are used to obtain the optimal parameters of SVM, and the SVM uses RBF kernel function. The range of kernel parameter is $[2^{-8}, 2^8]$. The range of penalization factor is $[2^{-8}, 2^8]$. Figure 5a, b, represents the classification by using the three polarimetric parameters and the polarimetric parameters after reducing dimension.

As is shown in Fig. 5, by using only a few polarimetric parameters may not obtain the correct classification result. The effect of classification with polarimetric features after reducing dimension is better, and it can distinguish the categories. In Fig. 5a, black wheat and coniferous forests cannot be distinguished, and some oat are divided into coniferous forests. So, reducing the dimension of multiple polarimetric data can improve the classification accuracy. The classification result of the SVM is not intuitive and affected greatly by noise. Therefore, it needs to be further processed.

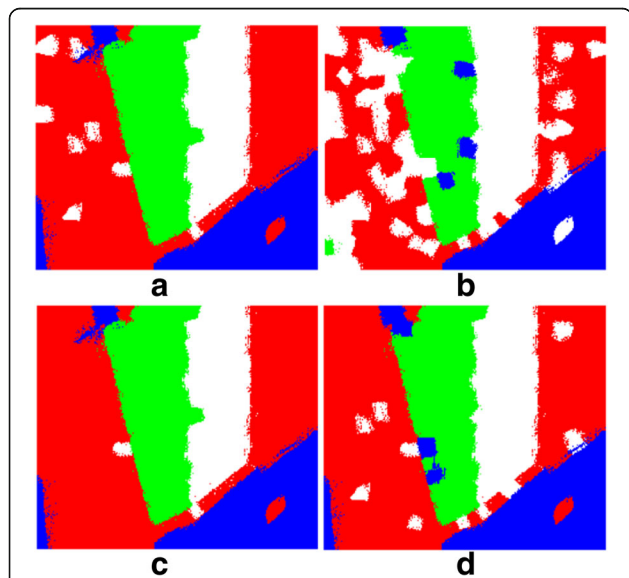


Fig. 9 The classification result of the PolSAR image by different dimension reduction methods. **a** PCA + SVM + superpixels. **b** LDA + SVM + superpixels. **c** LE + SVM + superpixels. **d** MVU + SVM + superpixels

5.2 The classification result of combining superpixels with majority voting principle

The result of the SVM classification is combined with superpixels to classify again. The parameter setting of superpixels affects the classification result directly. Only with optimal parameter can the optimal classification result be gained. Superpixel segmentation is decided by the superpixel block's side length a and the central point's perturbation range p . Figure 6 shows the superpixels generated with different parameters.

Figure 7 shows the result of classification by using the majority voting principle in the superpixel blocks, and the LE algorithm is used to reduce dimension.

Figure 8 shows the overall accuracy (OA) of Fig. 7. As is shown in Fig. 8, when $a = 14$, $p = 6$, the OA is the highest. So, the following analysis selects $a = 14$, $p = 6$ to conduct experiments.

Figure 9 shows the classification result of combining different dimension reduction methods with superpixels. The dimension reduction methods include PCA, LDA, LE, and MVU. Figure 10 shows the overall accuracy (OA) of Fig. 9.

Figure 10 shows the OA of classification with different dimension reduction methods. It can be seen that with LE dimension reduction, the best classification result is obtained.

6 Summary and conclusions

This paper proposes a PolSAR image classification method by using the improved superpixel segmentation and manifold learning. The method combines pixel information with spatial information for classification. The paper consists of four steps. Firstly, a 27-dimension polarimetric parameter vector is obtained from the polarimetric SAR data. Secondly, dimension reduction with LE algorithm is carried out on the polarimetric parameter vector. And then, pixels are classified by using the SVM method. At last, the superpixels are combined to classify the targets. This paper combines the LE method and MLE method to reduce dimension of data and the intrinsic structure in high-dimension data space can be found, and the dimension of feature parameter can be reduced. Moreover, the primary polarimetric information can be remained, and the polarimetric information can be utilized effectively. For the classification method, classifying superpixel blocks with majority voting principle is simple and effective, and it can reduce redundant information of high-resolution image and noise influence of SAR image. Moreover, it can save much computation for subsequent processing. On the whole, the classification method in this paper improves the visibility of classification result and makes the boundaries of the classified image more obvious. The classification effect is more accurate, and an accuracy rate over 90% can be reached.

Acknowledgements

The authors are grateful for the helpful insights provided by Dr. Jilan Feng.

Availability of data and materials

The datasets supporting the conclusions of this article are available at the web address <https://earth.esa.int/web/polsarpro/data-sources/sample-datasets>. The data can be read by the software PolSARpro which can be downloaded at the web address <https://www.ietr.fr/polsarpro/>.

Authors' contributions

HJW carried out polarimetric feature extraction on the polarimetric SAR data and reduced the dimension of feature space with Laplacian Eigenmap (LE) algorithm. JHH conducted the classification of PolSAR feature data after dimension reduction with SVM and obtained the superpixel segmentation.

YYD classified the superpixel blocks and analyzed the classification performance. All authors read and approved the final manuscript.

Funding

This research is funded by the Science and Technology Department of Sichuan Province (2016JY0106).

Competing interests

The authors declare that they have no competing interests.

Publisher's Note

Springer Nature remains neutral with regard to jurisdictional claims in published maps and institutional affiliations.

Received: 21 September 2017 Accepted: 14 November 2017

Published online: 21 November 2017

References

1. Y Wu, K Ji, W Yu, et al., Region-based classification of polarimetric SAR images using Wishart MRF[J]. *IEEE Geoscience & Remote Sensing Letters* 5(4), 668–672 (2008)
2. JJ Van Zyl, Unsupervised classification of scattering behavior using radar polarimetry data[J]. *IEEE Transactions on Geoscience & Remote Sensing* 27(1), 36–45 (1989)
3. SR Cloude, E Pottier, An entropy based classification scheme for land applications of polarimetric SAR[J]. *IEEE Transactions on Geoscience & Remote Sensing* 35(1), 68–78 (1997)
4. SR Cloude, E Pottier, A review of target decomposition theorems in radar polarimetry[J]. *IEEE Transactions on Geoscience & Remote Sensing* 34(2), 498–518 (1996)
5. E Krogager, New decomposition of the radar target scattering matrix[J]. *Electron. Lett.* 26(18), 1525–1527 (1990)
6. JA Kong, AA Swartz, HA Yueh, et al., Identification of terrain cover using the optimum polarimetric classifier[J]. *Journal of Electromagnetic Waves & Applications* 2(2), 171–194 (1988)
7. E Pottier, J Saillard, *On Radar Polarization Target Decomposition Theorems with Application to Target Classification, by Using Neural Network Method*[C], *Antennas and Propagation*, 1991. Icap 91. Seventh International Conference on. IET, vol 1 (2002), pp. 265–268
8. KS Chen, WP Huang, DH Tsay, et al., Classification of multifrequency polarimetric SAR imagery using a dynamic learning neural network[J]. *Geoscience & Remote Sensing IEEE Transactions on* 34(3), 814–820 (1996)
9. O Antropov, Y Rauste, H Astola, et al., Land cover and soil type mapping from Spaceborne PolSAR data at L-band with probabilistic neural network[J]. *IEEE Transactions on Geoscience & Remote Sensing* 52(9), 5256–5270 (2014)
10. S Fukuda, H Hirotsawa, *Support Vector Machine Classification of Land Cover: Application to Polarimetric SAR Data*[C], *Geoscience and Remote Sensing Symposium*, 2001. IGARSS '01. IEEE 2001 International. IEEE, vol 1 (2001), pp. 187–189
11. C He, S Li, Z Liao, et al., Texture classification of PolSAR data based on sparse coding of wavelet polarization textons[J]. *IEEE Transactions on Geoscience & Remote Sensing* 51(8), 4576–4590 (2013)
12. Zhong N, Yan T, Yang W, et al. A supervised classification approach for PolSAR images based on covariance matrix sparse coding[C]//*IEEE, International Conference on Signal Processing*. IEEE, (2017), pp. 213–216
13. M Tao, F Zhou, Y Liu, et al., Tensorial independent component analysis-based feature extraction for polarimetric SAR data classification[J]. *IEEE Transactions on Geoscience & Remote Sensing* 53(5), 2481–2495 (2015)
14. B Chen, S Wang, L Jiao, et al., A three-component fisher-based feature weighting method for supervised PolSAR image classification[J]. *IEEE Geoscience & Remote Sensing Letters* 12(4), 731–735 (2015)
15. A Masjedi, MJV Zoj, Y Maghsoudi, Classification of polarimetric SAR images based on modeling contextual information and using texture features[J]. *IEEE Transactions on Geoscience & Remote Sensing* 54(2), 932–943 (2016)
16. Chamundeeswari V V, Singh D, Singh K. An Analysis of Texture Measures in PCA-Based Unsupervised Classification of SAR Images[J]. *IEEE Geoscience & Remote Sensing Letters* 6(2):214–218 (2009)
17. JS Lee, MR Grunes, TL Ainsworth, et al., Unsupervised classification using polarimetric decomposition and the complex Wishart classifier[J]. *IEEE Transactions on Geoscience & Remote Sensing* 37(5), 2249–2258 (2002)

18. AP Doulgeris, SN Anfinen, T Eltoft, Classification with a non-Gaussian model for PolSAR data[J]. *IEEE Transactions on Geoscience & Remote Sensing* **46**(10), 2999–3009 (2008)
19. LQ Lin, H Song, PP Huang, et al., *Unsupervised Classification of PolSAR Data Using Large Scale Spectral Clustering*[C], Geoscience and remote sensing symposium. IEEE (2014), pp. 2814–2817
20. S Wang, K Liu, J Pei, et al., Unsupervised classification of fully polarimetric SAR images based on scattering power entropy and copolarized ratio[J]. *IEEE Geoscience & Remote Sensing Letters* **10**(3), 622–626 (2013)
21. G Liu, M Li, Y Wu, et al., PolSAR image classification based on Wishart TMF with specific auxiliary field[J]. *IEEE Geoscience & Remote Sensing Letters* **11**(7), 1230–1234 (2014)
22. AP Doulgeris, An automatic u-distribution and Markov random field segmentation algorithm for PolSAR images[J]. *IEEE Transactions on Geoscience & Remote Sensing* **53**(4), 1819–1827 (2014)
23. JS Lee, MR Grunes, E Pottier, et al., Unsupervised terrain classification preserving polarimetric scattering characteristics[J]. *Geoscience & Remote Sensing IEEE Transactions on* **42**(4), 722–731 (2004)
24. CT Chen, KS Chen, JS Lee, The use of fully polarimetric information for the fuzzy neural classification of SAR images[J]. *IEEE Transactions on Geoscience & Remote Sensing* **41**(9), 2089–2100 (2003)
25. KU Khan, J Yang, *Novel Features for Polarimetric SAR Image Classification by Neural Network*[C], International Conference on Neural Networks and Brain, 2005. *Icnn&b*. IEEE (2005), pp. 165–170
26. Yuan C, Casasent D. A new SVM for distorted SAR object classification[J]. In: *Proceedings of SPIE - The International Society for Optical Engineering*, (2005), 5816
27. H Cao, H Zhang, C Wang, et al., *Supervised Locally Linear Embedding for Polarimetric SAR Image Classification*[C], Geoscience and Remote Sensing Symposium (IGARSS), 2016 IEEE International. IEEE (2016), pp. 7561–7564
28. Agrawal N, Kumar S, Tolpekin V. Polarimetric SAR interferometry-based decomposition modelling for reliable scattering retrieval[C]// *SPIE Asia-Pacific Remote Sensing*, (2016), p. 987708
29. L Vincent, P Soille, Watersheds in digital spaces: an efficient algorithm based on immersion simulations[J]. *IEEE Transactions on Pattern Analysis & Machine Intelligence* **13**(6), 583–598 (1991)
30. Comaniciu D, Meer P. Mean Shift: A Robust Approach Toward Feature Space Analysis[M]. IEEE Computer Society, 2002.
31. R Achanta, A Shaji, K Smith, et al., SLIC superpixels compared to state-of-the-art superpixel methods[J]. *IEEE Transactions on Pattern Analysis & Machine Intelligence* **34**(11), 2274–2282 (2012)

Submit your manuscript to a SpringerOpen[®] journal and benefit from:

- Convenient online submission
- Rigorous peer review
- Open access: articles freely available online
- High visibility within the field
- Retaining the copyright to your article

Submit your next manuscript at ► springeropen.com
